


Interaction-induced directed transport in quantum chaotic subsystemsSanku Paul,^{1,*} J. Bharathi Kannan,^{2,†} and M. S. Santhanam^{2,‡}¹*Department of Physics and Astronomy, Michigan State University, East Lansing, Michigan 48824 USA*²*Department of Physics, Indian Institute of Science Education and Research, Pune 411008, India* (Received 8 July 2022; revised 28 March 2023; accepted 13 September 2023; published 9 October 2023; corrected 1 November 2023)

Quantum directed transport can be realized in noninteracting, deterministic, chaotic systems by appropriately breaking the spatiotemporal symmetries in the potential. In this work, the focus is on the class of *interacting* two-body quantum systems whose classical limit is chaotic. It is shown that one subsystem effectively acts as a source of “noise” to the other leading to intrinsic temporal symmetry breaking. Then, the quantum directed currents, even if prohibited by symmetries in the composite system, can be realized in the subsystems. This current is of quantum origin and does not arise from semiclassical effects. This protocol provides a minimal framework—broken spatial symmetry in the potential and presence of interactions—for realizing directed transport in interacting chaotic systems. It is also shown that the magnitude of directed current undergoes multiple current reversals upon varying the interaction strength and this allows for controlling the currents. It is explicitly demonstrated in the two-body interacting kicked rotor model. The interaction-induced mechanism for subsystem directed currents would be applicable to other interacting quantum systems as well.

DOI: [10.1103/PhysRevE.108.044208](https://doi.org/10.1103/PhysRevE.108.044208)**I. INTRODUCTION**

Basic physics teaches us that a particle can display directed motion only if it is acted upon by a net force $F \neq 0$. Ratchet effect is a counterintuitive phenomenon that arises as an exception to this general rule [1–4]. A diffusing particle, maintained away from equilibrium, can exhibit directed motion or ratchet effect even if the suitably averaged net force acting on it is zero, provided certain spatiotemporal symmetries are broken. This amounts to extracting useful work out of thermal fluctuations in *nonequilibrium* systems and is not prohibited by the second law of thermodynamics. Apart from clarifying the foundational principles of thermodynamics [2], ratchet mechanisms drive many biological processes—the intracellular transport of molecules along microtubules and movement of bacteria in a suspension fluid [5]. Such natural processes have inspired a plethora of ratchet models and experiments [3,6–17] in all the areas of physical sciences. This includes a general class of dissipative ratchets [3,4,18,19], electron ratchets [20,21], and recent applications for enhancing the efficiency of photovoltaic cells [22–24].

These developments have largely focused on exploiting thermal noise for extracting useful work. However, *noise-free* ratchets can also be created using Hamiltonian systems if they display chaotic dynamics. In these models, the inherent classical chaos formally plays the role of thermal noise within the framework of deterministic dynamics. This has

led to explorations of classical and quantum ratchets using chaotic Hamiltonian models such as the kicked rotor. In general, two distinct types of Hamiltonian models can generate directed currents. One approach requires bounded classical phase space and a coexistence of regular and chaotic dynamics [25–28]. These are subject to a semiclassical sum rule and directed momentum current arises due to the net difference between the currents carried by regular and chaotic phase space regions. In the $\hbar \rightarrow 0$ limit, this carries over to the quantum regime as well. The second approach accommodates nearly complete chaotic phase space and the external forcing must be suitably manipulated to break the temporal symmetry [29,30]. It supports saturated quantum ratchet current if dynamical localization occurs, with the quantum kicked rotor being a prime example. Another variant is the ratchet accelerators in which directed currents increase linearly with time under conditions of quantum resonance [31–33].

In the past two decades, the classical and quantum dynamics of single particle chaotic Hamiltonian ratchets were extensively studied [25,28,31,32,34]. In contrast, despite the exploding interest in interacting quantum many-body systems, ratchet dynamics in them largely remains unexplored [35,36]. Theoretical proposals based on periodically kicking the condensates indicate that the mean-field interactions can induce directed current [37,38]. Quantum directed current was also experimentally observed in a driven Bose-Einstein condensate in a toroidal trap when spatiotemporal symmetries were broken [39]. Recently, it was shown that quantum-classical correspondence in the ratchet regime differs from the generically expected delocalization of states and maximal entanglement applicable for a many-body quantum chaotic system [40,41].

In all these examples, the interacting atoms form a condensate represented by a macroscopic quantum state within

*sankup005@gmail.com. Current address: Department of Physics and Complex Systems, S.N. Bose National Centre for Basic Sciences, Kolkata 700106, India.

†jbarathi.kannan@students.iiserpune.ac.in

‡santh@iiserpune.ac.in

mean-field approximation. This implies that the subsystems—the individual atomic species—that constitute the condensate cannot be probed. Further, the time evolution of the condensate is governed by a *nonlinear* Schrödinger equation. Ironically, within the scope of *linear* quantum dynamics, the precise role of interactions and quantum chaos in generating directed currents remains unknown. In particular, it is not known if interactions generically enhance or suppress directed currents. Unlike condensates, interacting many-particle systems governed by a linear Schrödinger equation provide access to constituent subsystem dynamics. Then, a physically relevant question is the possibility to generate directed currents in the subsystems. In this work, we show that, in a classically chaotic interacting system, the interactions intrinsically break the temporal symmetry and generate directed quantum currents in the subsystems, even though the composite system might prohibit directed currents.

Another motivation arises from the fact that it is not easy to realize directed currents in a chaotic system, and even more difficult to sustain the currents. All the earlier realizations of directed currents in chaotic systems are either in a regime of mixed phase space [25–28] or require manipulation of an external kick sequence such as more than one kick in a cycle [29,30]. The latter approach is equivalent to changing the system itself. In contrast to these approaches, the interacting model presented in this work displays sustained directed currents without relying on mixed phase space or manipulated kick sequences. The ability to generate directed currents in a chaotic system without distorting the system of interest by applying additional fields is a question of considerable interest. Thus, in the spirit of this question, we emphasize that interactions provide a natural mechanism to realize and sustain directed currents in chaotic subsystems without the requirement of additional external fields to break temporal symmetry.

Hence we consider a simple prototype of a chaotic system composed of two interacting particles (regarded as subsystems), whose quantum dynamics is governed by a linear Schrödinger equation. Then, one of the subsystems plays the role of “environment” to the other [42]. Thus an interacting system effectively includes its own “environment,” implying that violation of spatial symmetries alone generates directed currents. This is because, as we analytically show below, the subsystem temporal symmetries are intrinsically broken by the interactions. There had been earlier works on convex billiards of constant width which display unidirectional motion due to peculiar interaction with the walls of billiard potential. Unlike our interacting model studied in this paper, this class of billiards (and also certain classes of reflectionless quantum graphs) provides examples of *single-particle* dynamics in which time-reversal symmetry is respected in the classical sense but is broken by quantum tunneling [43–46]. These are not interacting many-particle systems. For this class of systems, due to dynamically induced breaking of time-reversal symmetry in the quantum regime, the correspondence with random matrix level spacing distributions differ from what is expected based on the presence or absence of time-reversal symmetry.

Remarkably, the interacting models provide another paradigm for generating directed currents in quantum systems whose classical counterparts display complete chaos. It

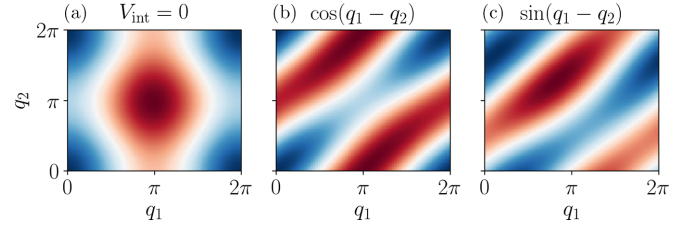


FIG. 1. [(a)–(c)] Image plot of the effective potential $V_{\text{eff}} = K_1 \cos q_1 + K_2 \cos q_2 + \varepsilon V_{\text{int}}(q_1, q_2)$ for $\varepsilon = 5$ and (a) $V_{\text{int}} = 0$, (b) $V_{\text{int}} = \cos(q_1 - q_2)$, and (c) $V_{\text{int}} = \sin(q_1 - q_2)$. Note that (c) lacks spatial symmetry. Parameters for CKR are $K_1 = 1.5$ and $K_2 = 0.8$.

discards the requirement of mixed classical phase space or manipulation of kick sequences or parameter sets for quantum resonances. To emphasize the generic nature, we demonstrate ratchet currents in two distinct interacting potentials; one obeys the assumptions of the Kolmogorov-Arnold-Moser (KAM) theorem [47], while the other violates one of the assumptions [48–51].

II. COUPLED KICKED ROTOR

We propose an interacting model as a natural candidate for realizing directed quantum currents. A general two-particle Hamiltonian of the form

$$H = H_1(q_1, p_1, t) + H_2(q_2, p_2, t) + \varepsilon V_{\text{int}}(q_1, q_2) f(t) \quad (1)$$

is considered, where $H_i(q_i, p_i, t)$ with $i = 1, 2$ represents a single-particle periodically kicked subsystem labeled 1 and 2 and $f(t) = \sum_{n=-\infty}^{\infty} \delta(t - n)$. The interaction potential $V_{\text{int}}(q_1, q_2)$ of strength ε is such that, if $\varepsilon = 0$, the system reduces to two independent noninteracting systems. In this paper, we show that, if $V_{\text{int}}(q_1, q_2)$ is chosen to break the spatial symmetry, then a directed quantum current emerges as a result of interactions without requiring an explicit temporal symmetry breaking. This is demonstrated in a chaotic coupled kicked rotor (CKR) model defined in a cylindrical phase space. The corresponding subsystem Hamiltonians, labeled by $i = 1$ and 2, are given by

$$H_i(q_i, p_i, t) = p_i^2/2 + K_i \cos q_i \sum_n \delta(t - n). \quad (2)$$

Kicked rotor is a well-studied model of Hamiltonian chaos [52–54] and corresponds to a particle receiving periodic kicks. In the quantum regime, a generic feature is the emergence of dynamical localization that suppresses classical diffusive dynamics for kick strengths $K \gg 1$. This is analogous to the Anderson localization observed in disordered lattices [55]. In this work, we fix the kick strengths of CKR as $K_1 = 1.5$ and $K_2 = 0.8$. To remain in the chaotic regime, the interaction strength is chosen to be $\varepsilon = 5$ since as $\varepsilon \rightarrow 0$ semiclassical effects arising in the near-integrable regime, rather than purely quantum effects, might drive the directed currents. By taking together kicking terms and interaction, the effective potential of the CKR turns out to be

$$V_{\text{eff}} = K_1 \cos q_1 + K_2 \cos q_2 + \varepsilon V_{\text{int}}(q_1, q_2). \quad (3)$$

Figures 1(a), 1(b) and 1(c) display the image plot of the effective potential V_{eff} of Eq. (3) corresponding to the

Hamiltonian in Eq. (1). For the kicking potentials in Eq. (2), three distinct cases arise: (i) no interactions, $\varepsilon = 0$, and spatial symmetry preserved [Fig. 1(a)], (ii) cosine interaction, $\varepsilon \neq 0$ and $V_{\text{int}}(q_1, q_2) = \cos(q_1 - q_2)$, and spatial symmetry maintained [Fig. 1(b)], and (iii) sine interaction, $\varepsilon \neq 0$ and $V_{\text{int}}(q_1, q_2) = \sin(q_1 - q_2)$, and spatial symmetry broken [Fig. 1(c)]. Thus we notice that, depending on the form of interaction, the spatial symmetry of the effective potential can be broken.

III. CLASSICAL DYNAMICS

The classical dynamics of CKR in Eq. (1) can be reduced to a stroboscopic map on a cylinder. The stroboscopic map is generated using the Hamilton equations of motion and for the CKR it is expressed as

$$\begin{aligned} p_1^{n+1} &= p_1^n + K_1 \sin(q_1^n) - \varepsilon \left. \frac{\partial V_{\text{int}}(q_1, q_2)}{\partial q_1} \right|_{q_1^n, q_2^n}, \\ p_2^{n+1} &= p_2^n + K_2 \sin(q_2^n) - \varepsilon \left. \frac{\partial V_{\text{int}}(q_1, q_2)}{\partial q_2} \right|_{q_1^n, q_2^n}, \\ q_1^{n+1} &= (q_1^n + p_1^{n+1}) \bmod 2\pi, \\ q_2^{n+1} &= (q_2^n + p_2^{n+1}) \bmod 2\pi, \end{aligned} \quad (4)$$

where q_i^n (p_i^n) represents the position (momentum) of the i th rotor at discrete time n with $i = 1, 2$. For sufficiently large kick strengths, the classical dynamics of CKR is strongly chaotic [54,56]. Further, chaos dominates even for small kick strengths if $\varepsilon \gg 1$ [57]. In this regime, the classical mean energy of either subsystem displays diffusive growth, i.e., $\langle E \rangle \sim D_{\text{cl}} n$, where D_{cl} is the classical diffusion coefficient.

The object of interest is the classical mean current in subsystem 1 denoted by $\langle p_1 \rangle^{\text{cl}}$, where $\langle \cdot \rangle$ represents averaging over initial conditions. To obtain $\langle p_1 \rangle^{\text{cl}}$, first let us consider the specific case of cosine interaction $V_{\text{int}}(q_1, q_2) = \cos(q_1 - q_2)$ in Eq. (4). Then, starting from the equation for p_1^{n+1} [in Eq. (4)] and by iterating over n from 0 to $N-1$, it can be rewritten in terms of initial conditions at $n = 0$ as

$$\begin{aligned} \sum_{n=0}^{N-1} p_1^{n+1} - p_1^0 &= p_1^{N+1} - p_1^0 \\ &= K_1 \sum_{n=0}^{N-1} \sin q_1^n - \varepsilon \sum_{n=0}^{N-1} \sin(q_1^n - q_2^n). \end{aligned} \quad (5)$$

By dividing throughout by N and taking the limit $N \rightarrow \infty$, this reduces to

$$\langle p_1 \rangle = K_1 \langle \sin q_1 \rangle - \varepsilon \langle \sin q_1 \cos q_2 \rangle + \varepsilon \langle \cos q_1 \sin q_2 \rangle. \quad (6)$$

Under conditions of chaotic dynamics and in the absence of terms that could break time-reversal symmetry in the equation of motion, each of the averages on the right hand side vanishes and hence we obtain that $\langle p_1 \rangle = 0$. By the same argument, classical mean momentum vanishes even for $V_{\text{int}}(q_1, q_2) = \sin(q_1 - q_2)$.

Figure 2 shows the classical mean current $\langle p_1 \rangle^{\text{cl}}$ simulated using Eq. (4). This current fluctuates about $\langle p_1 \rangle^{\text{cl}} = 0$ and indicates the absence of the net classical current for both the interacting and noninteracting cases. The magnitude of these

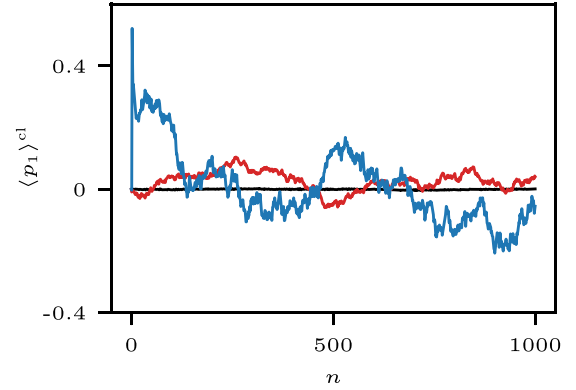


FIG. 2. Absence of averaged classical current $\langle p_1 \rangle^{\text{cl}}$ is shown for CKR and for three different interaction potentials with $\varepsilon = 5$: (i) noninteracting ($V_{\text{int}} = 0$) (black curve), (ii) $V_{\text{int}} = \cos(q_1 - q_2)$ (red), and (iii) $V_{\text{int}} = \sin(q_1 - q_2)$ (blue). The averaging is done over 10^6 initial samples taken from an interval $q_i \in [0, 2\pi]$ and $p_i = 0$. Other parameters are $K_1 = 1.5$ and $K_2 = 0.8$.

fluctuations about $\langle p_1 \rangle^{\text{cl}} = 0$ can be reduced by increasing the number of initial conditions used to estimate the average classical current. In Fig. 2, though it might appear that $\langle p_1 \rangle^{\text{cl}} \neq 0$, due to the frequent reversals of current direction it cannot be regarded as a sustained directed current in one particular direction. The absence of such a *sustained* net classical current is due to the presence of near-complete chaos in the system and the absence of an explicit temporal symmetry breaking term in the effective potential, V_{eff} . Thus, in a classically chaotic interacting system, without a temporal symmetry breaking, a sustained net directed current is not generated. As we show in the rest of this paper, notwithstanding the absence of a classical directed current, it is possible to realize sustained directed currents in the quantum regime.

IV. DIRECTED QUANTUM TRANSPORT

Quantum dynamics of the CKR in Eq. (1) can be conveniently generated by the unitary period-1 time-evolution operator $\mathcal{U} = (U_1 \otimes U_2)U_{\text{int}}$, where $U_i = e^{-iH_i/\hbar_s}$ with $i = 1, 2$ represents the evolution operator for subsystems 1 and 2, respectively, while $U_{\text{int}} = e^{-i\varepsilon \frac{V_{\text{int}}}{\hbar_s}}$ arises from the interaction and \hbar_s is the scaled Planck constant which is set to 1 throughout this paper. With kicked rotor in Eq. (2) as subsystems, the evolution operator can be decomposed as $U_i = U_i^{\text{free}}(p_i)U_i^{\text{kick}}$, with $i = 1, 2$ labeling the respective subsystems. In this, $U_i^{\text{free}}(p_i)$ and U_i^{kick} correspond, respectively, to free propagation part and kicking part. In numerical simulations, an arbitrary initial state is evolved using the split operator technique, which is exact in this case due to time dependence in the form of a delta function term. This technique requires applying one fast Fourier transform and its inverse in every iteration to transform from position to momentum representation and back [58]. In Eq. (2) due to spatial periodicity of the potential, momentum p_i takes values $p_i = (n_i + \beta_i)$, with $n_i \in \mathbb{Z}$ and β_i being the conserved quasimomentum for subsystems labeled $i = 1, 2$. The operator U_i^{free} is the free evolution operator, while U_i^{kick} corresponds to the kicking part. The dynamics at later time is generated by operating

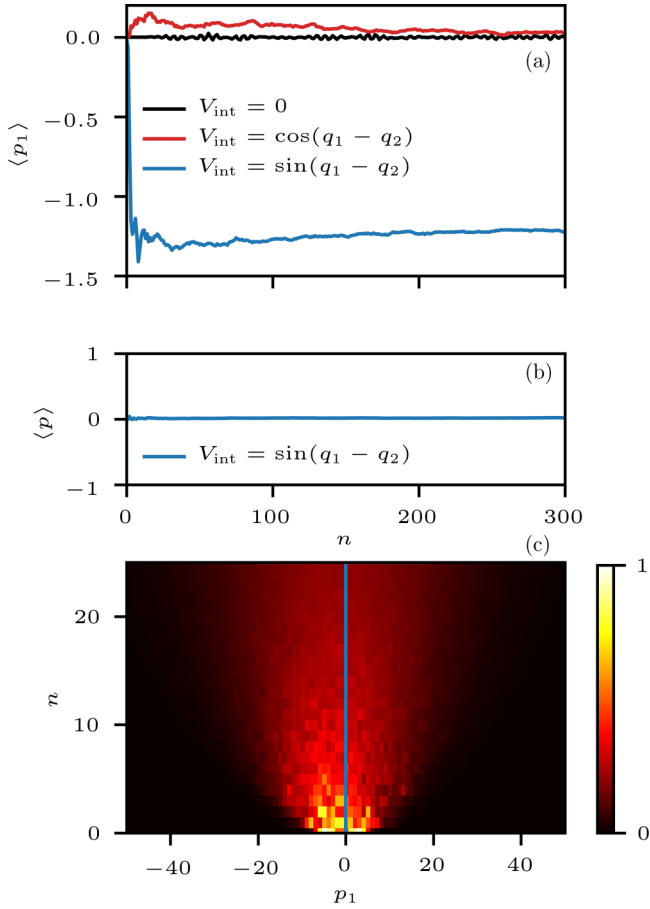


FIG. 3. (a) Mean current $\langle p_1 \rangle$ in subsystem 1 for CKR with $V_{\text{int}} = 0$ (black line), $V_{\text{int}} = \cos(q_1 - q_2)$ (red), and $V_{\text{int}} = \sin(q_1 - q_2)$ (blue). (b) Plot shows current $\langle p \rangle$ in composite CKR as a function of time. These numerical results are averaged over 200 quasimomenta β chosen randomly in the interval $[-0.1, 0.1]$. (c) Time evolving momentum distribution $f(p_1)$ (scaled by its peak value) is shown for $V_{\text{int}} = \sin(q_1 - q_2)$. Vertical blue line at $p_1 = 0$ is a guide to the eye. Parameters for CKR are $K_1 = 1.5$, $K_2 = 0.8$, $\varepsilon = 5$, and subsystem basis size, $N = 2^{11}$.

\mathcal{U} on an initial state $|\psi(0)\rangle$ to get the time evolved state $|\psi(t)\rangle = \mathcal{U}^t |\psi(0)\rangle$.

In the following, the initial state is chosen to be a direct-product state $|\psi(0)\rangle = |\phi_1(0)\rangle \otimes |\phi_2(0)\rangle$, where $|\phi_i(0)\rangle = 1/\sqrt{2\pi}$ ($i = 1, 2$) is a zero momentum state. We focus on the generation of mean current $\langle p_1 \rangle$ in subsystem 1 evaluated as $\langle p_1 \rangle = \langle \psi(n) | p_1 | \psi(n) \rangle$. The mean current in the *composite* system is denoted by $\langle p \rangle = \langle p_1 + p_2 \rangle$.

For the three distinct interaction potentials shown in Fig. 1, Fig. 3(a) displays the respective $\langle p_1 \rangle$. Surprisingly, even in the absence of explicit temporal symmetry breaking in the system, subsystem directed current, $\langle p_1 \rangle \neq 0$, emerges in the case of sine interactions that breaks spatial symmetry while, for the other interaction potentials with spatial symmetry preserved, directed current is absent, $\langle p_1 \rangle = 0$. The directed current in the composite system $\langle p \rangle = \langle p_1 + p_2 \rangle$ also vanishes with the identical symmetry-breaking sine interactions as shown in Fig. 3(b). The absence of mean current $\langle p \rangle$ can be attributed to the lack of temporal symmetry breaking in the composite

system. Thus Figs. 3(a) and 3(b) indicate that subsystem directed currents can be intrinsically engineered—even in the absence of directed currents in the composite system—by appropriate choice of interaction potential *without* requiring explicit temporal symmetry breaking.

The time evolving subsystem momentum distribution $f(p_1)$ for $V_{\text{int}}(q_1, q_2) = \sin(q_1 - q_2)$ is shown in Fig. 3(c). The quantity $f(p_1)$ is the diagonal elements of the reduced density matrix of the subsystem 1. The distributions lack symmetry about any arbitrary reference value. The asymmetry freezes quickly leading to a saturated directed current seen in Fig. 3(a). The sign of the generated current—negative in these cases in Fig. 3(a)—depends on the choice of parameters.

V. BROKEN TIME-REVERSAL SYMMETRY

A natural question is about the mechanism that generates such subsystem directed quantum current even if prohibited by symmetries in the corresponding composite system. As we demonstrate below, in the chaotic limit, one subsystem acts as a source of “noisy environment” to the other, leading to temporal symmetry breaking at subsystem level but not in the composite system. This can be seen as follows. By using trigonometric identity to expand $V_{\text{int}}(q_1, q_2) = \sin(q_1 - q_2)$ and rearranging terms, the effective potential becomes

$$V_{\text{eff}} = \cos q_1 (K_1 - \varepsilon \sin q_2) + \cos q_2 (K_2 + \varepsilon \sin q_1). \quad (7)$$

By isolating the terms within the brackets, an effective kicking strength for the i th subsystem can be identified as

$$K_i^{\text{eff}} = K_i + (i - j)\varepsilon \sin q_j, \quad j = 1, 2, i \neq j, \quad (8)$$

indicating that subsystem i receives inputs from subsystem j through $\varepsilon \sin q_j$ (and vice versa). The numerical simulations in Fig. 4(a) show that, if the subsystem is chaotic, then $\kappa_n = \langle \psi(n) | \varepsilon \sin q_j | \psi(n) \rangle$ is effectively a “noisy” process. In particular, its autocorrelation function is $C_m = \langle \kappa_n \kappa_{n+m} \rangle \sim A \delta(m)$ (A is a constant), representing an uncorrelated process [see inset in Fig. 4(a)]. Hence, due to interactions, one subsystem is driven by the noisy dynamics of the other. This effectively breaks the temporal symmetry in the subsystems. The role of chaos is to provide a source of “uncorrelated noise” to the other subsystem. In the absence of chaos, it is not clear if the terms “directed current” or “ratchet currents” can be used for net currents (assuming it exists) when the system is in a near-integrable regime because in such cases the directed net current does not result from a “fluctuating environment.”

To demonstrate that the interactions induce breaking of time-reversal symmetry, the following sequence of operations are performed: the initial state is evolved forward for duration $\tau > 0$ under the action of H in Eq. (1). Next, subsystem 1 is evolved backward in time for duration $-\tau$, while subsystem 2 is evolved forward for duration τ . This sequence of operations can be represented as

$$|\psi(\tau')\rangle = [(U_1^{-\tau} \otimes U_2^\tau) U_{\text{int}}^\tau] [(U_1 \otimes U_2) U_{\text{int}}]^\tau |\psi(0)\rangle. \quad (9)$$

In this, τ' indicates successive time duration of $(\tau, -\tau)$ for subsystem 1 and (τ, τ) for subsystem 2. Let $\rho(\tau') = |\psi(\tau')\rangle \langle \psi(\tau')|$ be the associated density matrix and the reduced density matrix for subsystem 1 is $\rho_1(\tau') = \text{Tr}_2 \rho(\tau')$. Due to unitary evolution, we might expect subsystem 1

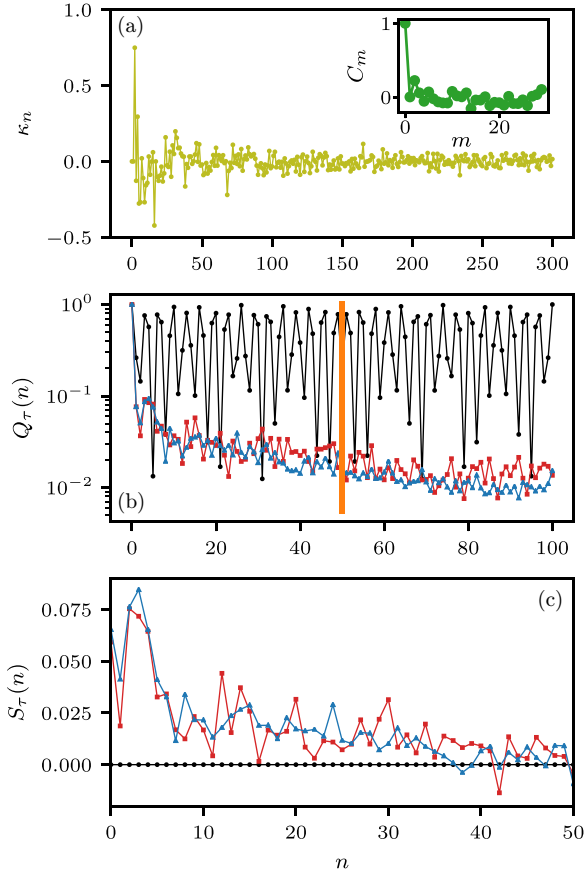


FIG. 4. (a) Time series of $\kappa_n = \langle \psi(n) | \varepsilon \sin q_j | \psi(n) \rangle$. The insets show the numerically computed autocorrelation function $C_m = \langle \kappa_n \kappa_{n+m} \rangle$. (b) $Q_\tau(n)$ with no interaction $\varepsilon = 0$ (black symbols), with interactions $V_{\text{int}} = \cos(q_1 - q_2)$ (red) and $V_{\text{int}} = \sin(q_1 - q_2)$ (blue). The vertical orange line indicates $n = \tau$ about which time-reversal symmetry is expected. (c) $S_\tau(n)$ indicating the existence or absence of time-reversal symmetry about $n = \tau$. Note that temporal symmetry is preserved if $\varepsilon = 0$ and it is broken for $\varepsilon \neq 0$. All the other parameters are the same as in Fig. 3.

to retrace its path to the initial state. As shown exactly in Appendix A 1, this expectation is true in the absence of interactions ($\varepsilon = 0$). Using the definition $Q_\tau(n) = \langle \phi_1(0) | \rho_1(n) | \phi_1(0) \rangle$, we have that $Q_\tau = 1$. In this case, existence of temporal symmetry about $n = \tau$ implies precise time reversal, i.e.,

$$Q_\tau(n) = Q_\tau(2\tau - n), \quad n = 1, 2, \dots, \tau. \quad (10)$$

If the interaction is present for $\varepsilon \neq 0$, it can be exactly shown that (in Appendix A 2)

$$0 < Q_\tau(n = \tau') = \langle \phi_1(0) | \rho_1(\tau') | \phi_1(0) \rangle < 1. \quad (11)$$

Indeed, $Q_\tau(n) \neq Q_\tau(2\tau - n)$, confirming that interactions induce time-reversal symmetry violation. It is a general feature of interacting subsystems and not specific to kicked models alone.

The numerical simulations for CKR shown in Fig. 4 explicitly demonstrate the lack of temporal symmetry if $\varepsilon \neq 0$. Figure 4(b) with $\tau = 50$ shows $Q_{50}(n)$ for $n = 1, 2, \dots, 2\tau$ iterations. With $\varepsilon = 0$ (black circles), under time reversal, the

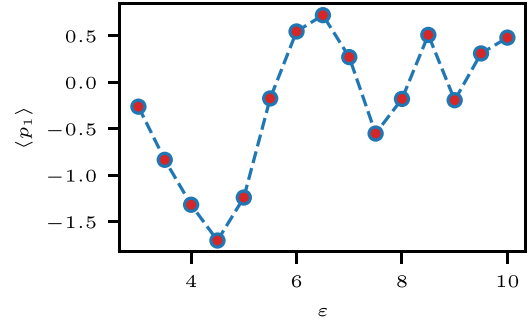


FIG. 5. Quantum current $\langle p_1 \rangle$ generated at fixed time $n = 200$ by CKR as a function of coupling strength ε . Other parameters are the same as in Fig. 3.

state of subsystem 1 retraces its path to the initial state. In particular, the time evolution is symmetric about $\tau = 50$ (marked as a magenta line). In contrast, if $\varepsilon \neq 0$, then $Q_{50}(100) < 1$ and temporal symmetry is absent. Figure 4(c) shows a diagnostic measure

$$S_\tau(n) = Q_\tau(n) - Q_\tau(2\tau - n), \quad n = 1, 2, \dots, \tau, \quad (12)$$

to reveal the existence or absence of temporal symmetry. Clearly, $S_\tau(n) = 0$ if temporal symmetry about $n = \tau$ is present, while $S_\tau(n) \neq 0$ if this symmetry is absent. As seen in Fig. 4(c), $S_\tau(n) = 0$ for $\varepsilon = 0$ and $S_\tau(n) \neq 0$ for $\varepsilon \neq 0$. With appropriate choice of symmetry-broken interaction $V_{\text{int}}(q_1, q_2)$, generically, the directed quantum current will be generated in subsystems as shown in Fig. 3(a).

To obtain a global perspective on the directed quantum currents in subsystem 1, Fig. 5 displays mean current $\langle p_1 \rangle$ after $n = 200$ iterations as a function of coupling strength ε . For this plot, we restrict to the interaction potential $V_{\text{int}} = \sin(q_1 - q_2)$ that breaks the spatial symmetry. It is clear that in the absence of spatiotemporal symmetries, generically, for any $\varepsilon \gg 0$, directed currents are generated in the subsystem. Even so, the currents are not guaranteed to be sufficiently large. It might be emphasized that the term “generically” does not rule out exceptional points at which mean currents could vanish despite the broken spatiotemporal symmetries. Barring such exceptional points, the generated currents are robust and can be controlled by tuning the interaction strength ε . However, as Fig. 5 reveals, the currents do not show a systematic relationship with ε . Previous studies on quantum ratchets and accelerators have observed such a nonsystematic relationship between current and a system parameter [59–63] and are attributed to choice of initial states, effects due to tiny regular classical regions in phase space, and changes in the effective Planck’s constant as a parameter is varied. A deeper understanding of the net currents (such as shown in Fig. 5) in a chaotic regime based on statistical approaches requires special choice of initial states (as done in Ref. [63]) and a general theoretical framework is absent for an arbitrary choice of localized initial states. Thus the interactions provide a minimal framework—requiring only broken spatial symmetry—to realize a directed quantum current in subsystems.

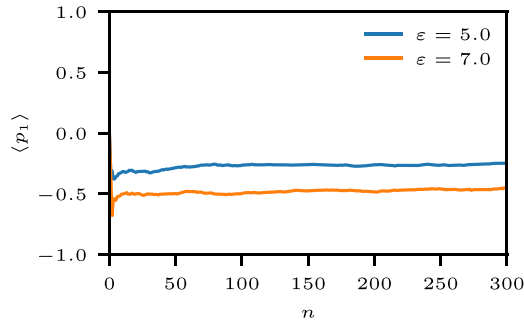


FIG. 6. Mean quantum current $\langle p_1 \rangle$ shown as a function of time for the interaction potential $V_{\text{int}} = -2\varepsilon|q_1||q_2|$ in the system represented by Eq. (1). Other parameters are the same as in Fig. 3.

Nonanalytic interaction potential

We emphasize that the results presented here are general and not specific to the choice of V_{eff} , except for the requirement that V_{eff} must break the spatial symmetry. To underscore this point, Fig. 6 displays quantum currents obtained for $V_{\text{eff}}(q_1, q_2) = K_1 \sin q_1 + K_2 \sin q_2 + V_{\text{int}}$, where $V_{\text{int}} = -2\varepsilon|q_1||q_2|$. This interaction potential is nonanalytic and violates one of the assumptions of the KAM theorem (non-KAM system) [49–51]. The classical limit of this system is chaotic and the interaction breaks the spatial symmetry of the potential. As shown in Fig. 6, $\langle p_1 \rangle \neq 0$ in this case as well. This illustrates that, generically, a directed quantum current in the subsystem is generated as long as spatial symmetry of the interacting system is broken. Throughout this work, we have demonstrated quantum currents generated by subsystem 1, though similar results would be obtained had subsystem 2 been chosen.

VI. CONCLUSIONS

Directed currents are usually generated if the relevant spatiotemporal symmetries in the potential are explicitly broken. In the earlier results on chaotic quantum ratchets, especially in the context of kicked systems, this condition was met by manipulating both the potential and the kick sequences. In contrast, we have shown that, for a classically chaotic *interacting* quantum system, explicitly breaking the spatial symmetry alone can generate directed currents in the subsystems. This is achieved without modifying the potential or the kick sequences at the subsystem level and the only requirement is that the subsystems display chaotic dynamics. This provides a natural framework to realize directed currents in subsystems using interactions to break the temporal symmetry. As shown analytically, the time-reversal symmetry breaking is *intrinsically* induced by the interaction potential acting between the two subsystems. Effectively, one part of the system acts as the “environment” for the other and subsystem directed currents can exist even if the directed quantum currents are absent in the composite system.

This is demonstrated in a chaotic coupled system—namely, the coupled kicked rotor in a regime of predominant classical chaos. Thus chaos in the subsystems and presence of interactions among them leads to directed quantum currents, even when the classical currents average to zero. The current

arises from purely quantum rather than semiclassical effects in the integrable or near-integrable regimes. Another significant feature is the tunability of the directed current. For any proposal for directed currents, tunability is an important criteria. We have shown through simulations that by varying the interaction strength ε multiple current reversals take place, i.e., current changes sign multiple times. This implies that directed currents arise over a large range of parameters. Further, this provides a mechanism to tune for and obtain a desired magnitude of directed current.

This interaction induced mechanism is sufficiently general and would also be applicable to other interacting quantum systems. As shown in this paper, this mechanism for generating directed currents in the quantum domain works even for the interacting potential that is nonanalytic in nature. We believe that it might be feasible to realize a coupled kicked rotor in experiments by subjecting atomic matter waves to flashing incommensurate optical lattices; the interactions arise during the free evolution when the lattices are off [64,65].

The presence of classical chaos provides the required “stochasticity” in the problem. Yet, it will be of interest to explore the question of directed currents when one of the subsystems is not chaotic. While the interactions will induce temporal symmetry breaking, studying subsystems with various degrees of nonintegrability will give further insights into the crucial role played by chaotic dynamics in generating subsystem directed currents. Given the earlier debates on this topic, this will also help refine our ideas on what constitutes a ratchet current. Finally, we might also remark that this approach for directed currents for a two-particle system can be extended to interacting many particle systems that display chaotic dynamics. In the backdrop of current interests in chaotic many-particle systems (for example, see Ref. [66] for a closely related phenomenon dubbed as the boomerang effect), these studies might add other possibilities for dynamical phases in such systems.

ACKNOWLEDGMENTS

M.S.S. would like to acknowledge the support from MATRICS Grant No. MTR/2019/001111 of SERB, DST, Govt of India. S.P. is supported by the start-up funding from Michigan State University and funding from DST, India. J.B.K. and M.S.S. thank the QuEST programme of DST and also the I-HUB Quantum Technology Foundation for partial funding in support of this project.

APPENDIX: TIME-REVERSAL SYMMETRY BREAKING

Let us consider a coupled system consisting of two subsystems which are interacting with one another. In this section, we analytically show the effect of interaction in breaking the time-reversal symmetry of a subsystem in the presence of the other. The formalism introduced is general, not limited to the models considered in the main paper, and can be extended to many-body systems as well. To begin with, let us first understand the situation in the absence of interaction and then discuss the role of interaction in time-reversal symmetry breaking. The subsequent subsections discuss both situations.

1. Without interaction

Here, we discuss the time-reversal symmetry of the individual subsystems in the absence of interactions. To this end, we consider the initial state $|\psi(0)\rangle$ of the interacting system at time $t = 0$ to be a product state of the subsystems

$$|\psi(0)\rangle = |\phi_1(0)\rangle \otimes |\phi_2(0)\rangle = \sum_i a_i |i\rangle_1 \otimes \sum_j b_j |j\rangle_2, \quad (\text{A1})$$

where $|i\rangle_1$ ($|j\rangle_2$) represents the basis of subsystem 1 (subsystem 2). The coefficients a_i (b_j) satisfy the normalization condition $\sum_i |a_i|^2 = 1$ ($\sum_j |b_j|^2 = 1$).

In the case of an uncoupled system, the time evolution operator of the entire system \mathcal{U} can be written as the tensor product of the individual unitary time evolution operators U_1 and U_2 at all times

$$\mathcal{U} = U_1 \otimes U_2. \quad (\text{A2})$$

The time evolved state of the composite system at time $\tau > 0$ is given by

$$|\psi(\tau)\rangle = \mathcal{U}^\tau |\psi(0)\rangle = U_1^\tau |\phi_1(0)\rangle \otimes U_2^\tau |\phi_2(0)\rangle. \quad (\text{A3})$$

If a subsystem has a time-reversal symmetry, the exact initial state of the subsystem can be obtained by evolving the subsystem backward in time for $t = -\tau$. Thus, to examine the time-reversal symmetry of the subsystem 1 in the presence of subsystem 2, we evolve subsystem 1 backward in time for the duration $-\tau$, while the subsystem 2 is evolved forward for duration τ ; the state obtained is

$$\begin{aligned} |\psi(\tau')\rangle &= (U_1^{-\tau} \otimes U_2^\tau) |\psi(\tau)\rangle \\ &= (U_1^{-\tau} \otimes U_2^\tau) U_1^\tau |\phi_1(0)\rangle \otimes U_2^\tau |\phi_2(0)\rangle \\ &= U_1^{-\tau} U_1^\tau |\phi_1(0)\rangle \otimes U_2^\tau U_2^\tau |\phi_2(0)\rangle \\ &= |\phi_1(0)\rangle \otimes |\phi_2(2\tau)\rangle. \end{aligned} \quad (\text{A4})$$

The density matrix of the composite system at τ' [where τ' indicates successive time duration of $(\tau, -\tau)$ for subsystem 1 and (τ, τ) for subsystem 2] can be estimated using the time evolved state obtained in (A4) and is expressed as

$$\rho(\tau') = |\psi(\tau')\rangle \langle \psi(\tau')| = |\phi_1(0)\rangle \langle \phi_1(0)| \otimes |\phi_2(2\tau)\rangle \langle \phi_2(2\tau)|. \quad (\text{A5})$$

The reduced density matrix of the subsystem 1 can be obtained from $\rho(\tau')$ by tracing out the subsystem 2 at τ' and is given by

$$\begin{aligned} \rho_1(\tau') &= \text{Tr}_2[\rho(\tau')] \\ &= \sum_j \langle j | \phi_1(0)\rangle \langle \phi_1(0) | \otimes |\phi_2(2\tau)\rangle \langle \phi_2(2\tau) | j \rangle_2 \\ &= |\phi_1(0)\rangle \langle \phi_1(0) | \otimes \sum_j \langle j | \sum_{j', j''} b_{j'}(2\tau) b_{j''}^*(2\tau) | j' \rangle_2 \\ &\quad \times \langle j'' | j \rangle_2 \\ &= |\phi_1(0)\rangle \langle \phi_1(0) | \sum_j |b_j(2\tau)|^2 \\ &= |\phi_1(0)\rangle \langle \phi_1(0) |, \end{aligned} \quad (\text{A6})$$

where $b_j = \langle j | \phi_2(2\tau)\rangle$ and $\sum_j |b_j(2\tau)|^2 = 1$. Now, to investigate the time-reversal symmetry, we calculate the expectation value of $\rho_1(\tau')$ with respect to the initial state of the subsystem 1. In this paper, we call this quantity $Q_\tau(n) = \langle \phi_1(0) | \rho_1(n) | \phi_1(0)\rangle$. Evaluating $Q_\tau(n = \tau')$ leads to

$$\langle \phi_1(0) | \rho_1(\tau') | \phi_1(0)\rangle = \langle \phi_1(0) | \phi_1(0)\rangle \langle \phi_1(0) | \phi_1(0)\rangle = 1. \quad (\text{A7})$$

$Q_\tau(n = \tau') = 1$ implies that subsystem 1 retraces its path to the initial state after time τ' . Thus we see that the time-reversal symmetry is preserved in subsystem 1 in the presence of subsystem 2. This is an expected result as there is no interaction between the subsystems and is also a property of unitary evolution. Using a similar formalism discussed above, it can be shown that time-reversal symmetry is preserved in subsystem 2 in the presence of subsystem 1.

2. With interaction

In this subsection, we show that the interaction between two subsystems breaks the time-reversal symmetry of the individual subsystems. For that, consider the initial state at time $t = 0$ of the interacting system to be a product state,

$$\begin{aligned} |\psi(0)\rangle &= |\phi_1(0)\rangle \otimes |\phi_2(0)\rangle = \sum_i a_i |i\rangle_1 \otimes \sum_j b_j |j\rangle_2 \\ &= \sum_{i,j} c_{ij}(0) |i, j\rangle, \end{aligned} \quad (\text{A8})$$

where a_i , $|i\rangle_1$, b_j , and $|j\rangle_2$ have the same meaning as in (A1).

The time evolution operator for the interacting system of two subsystems can be written as

$$\mathcal{U} = (U_1 \otimes U_2) U_I, \quad (\text{A9})$$

where U_1 and U_2 are the time evolution operators for subsystem 1 and subsystem 2, respectively, and U_I is the unitary time evolution operator corresponding to the interaction between the subsystems. The time evolved state at τ is given by

$$\begin{aligned} |\psi(\tau)\rangle &= \mathcal{U}^\tau |\psi(0)\rangle = [(U_1 \otimes U_2) U_I]^\tau \sum_{i,j} c_{ij}(0) |i, j\rangle \\ &= \sum_{i,j} d_{ij}(\tau) |i, j\rangle. \end{aligned} \quad (\text{A10})$$

Now, to investigate if the time-reversal symmetry of the subsystem 1 in the presence of subsystem 2 is broken or not, we evolve subsystem 1 backward in time, i.e., $-\tau$, while subsystem 2 and the interaction term move forward for the same time τ . The evolved state thus obtained is

$$\begin{aligned} |\psi(\tau')\rangle &= (U_1^{-\tau} \otimes U_2^\tau) U_I^\tau |\psi(\tau)\rangle \\ &= [(U_1^{-\tau} \otimes U_2^\tau) U_I^\tau] [(U_1 \otimes U_2) U_I]^\tau \sum_{i,j} c_{ij}(0) |i, j\rangle \\ &= [U_1^0 \otimes U_2^{2\tau}] U_I^{2\tau} \sum_{i,j} c_{ij}(0) |i, j\rangle \\ &= \sum_{i,j} d_{ij}(\tau') |i, j\rangle. \end{aligned} \quad (\text{A11})$$

The density matrix of the total system at τ is given by

$$\rho(\tau') = |\psi(\tau')\rangle\langle\psi(\tau')| = \sum_{i,j,i',j'} d_{ij}(\tau') d_{i'j'}^*(\tau') |i, j\rangle\langle i', j'|. \quad (\text{A12})$$

The reduced density matrix of subsystem 1 obtained by tracing out subsystem 2 from the total density matrix $\rho(\tau')$ in (A12) is

$$\begin{aligned} \rho_1(\tau') &= \text{Tr}_2[\rho(\tau')] \\ &= \sum_{j''} {}_2\langle j''| \sum_{i,j,i',j'} d_{ij}(\tau') d_{i'j'}^*(\tau') |i, j\rangle\langle i', j'| j''\rangle_2 \\ &= \sum_{i,i'} {}_1\langle i|i'\rangle_1 \sum_j d_{ij}(\tau') d_{i'j}^*(\tau'). \end{aligned} \quad (\text{A13})$$

Now to understand if the time-reversal symmetry is preserved or not, we evaluate $Q_\tau(\tau') = \langle\phi_1(0)|\rho_1(\tau')|\phi_1(0)\rangle$, which is

$$\begin{aligned} Q_\tau(\tau') &= \sum_{i''} a_{i''}^*(0) {}_1\langle i''| \sum_{i,i'} |i\rangle_1 {}_1\langle i'| \\ &\quad \times \sum_j d_{ij}(\tau') d_{i'j}^*(\tau') \sum_{i'''} a_{i'''}(0) |i'''\rangle_1 \end{aligned}$$

$$\begin{aligned} &= \sum_{i'',i',i'''} a_{i''}^*(0) a_{i'''}(0) {}_1\langle i''|i\rangle_1 \langle i'|i'''\rangle_1 \\ &\quad \times \sum_j d_{ij}(\tau') d_{i'j}^*(\tau') \\ &= \sum_{i,i'} a_i^*(0) a_i(0) \sum_j d_{ij}(\tau') d_{i'j}^*(\tau') \\ &\leq 1. \end{aligned} \quad (\text{A14})$$

In this last equation, equality holds if there is no interaction between the subsystems. Otherwise, $Q_\tau(n = \tau') < 1$. This implies that, in the presence of interaction, subsystem 1 does not retrace its path to the initial state after time τ' . This indicates that the time-reversal symmetry is broken in subsystem 1 due to the interaction between the subsystems. In fact, this inequality, $Q_\tau(n = \tau') < 1$, is very general and holds true at the subsystem level for any interacting system. This can be understood in the following sense: that the subsystem dynamics is governed by a nonunitary operator and, being a non-Hamiltonian dynamics, the subsystem displays irreversibility. If the dynamics is chaotic, then one subsystem provides an uncorrelated noise to the other and effectively acts as a noisy environment. Owing to this property, even in the chaotic limit without an explicit time-reversibility breaking term, we observe ratchet effect.

-
- [1] M. Smoluchowski, *Pis'ma Mariana Smoluchowskiego* **2**, 226 (1927).
- [2] R. P. Feynman, R. B. Leighton, and M. Sands, *Feynman Lectures on Physics, Vol. 1* (Addison-Wesley, Redwood City, CA, 1966).
- [3] P. Reimann, *Phys. Rep.* **361**, 57 (2002).
- [4] P. Hänggi and F. Marchesoni, *Rev. Mod. Phys.* **81**, 387 (2009).
- [5] R. D. Astumian, *Phys. Chem.* **9**, 5067 (2007).
- [6] F. Jülicher, A. Ajdari, and J. Prost, *Rev. Mod. Phys.* **69**, 1269 (1997).
- [7] V. Bermudez, N. Capron, T. Gase, F. G. Gatti, F. Kajzar, D. A. Leigh, F. Zerbetto, and S. Zhang, *Nature (London)* **406**, 608 (2000).
- [8] J. E. Villegas, S. Savel'ev, F. Nori, E. M. Gonzalez, J. V. Anguita, R. García, and J. L. Vicent, *Science* **302**, 1188 (2003).
- [9] P. Hänggi, F. Marchesoni, and F. Nori, *Ann. Phys. (NY)* **517**, 51 (2005).
- [10] L. Sanchez-Palencia, *Phys. Rev. E* **70**, 011102 (2004).
- [11] P. Sjölund, S. J. H. Petra, C. M. Dion, S. Jonsell, M. Nylén, L. Sanchez-Palencia, and A. Kastberg, *Phys. Rev. Lett.* **96**, 190602 (2006).
- [12] V. Serreli, C.-F. Lee, E. R. Kay, and D. A. Leigh, *Nature (London)* **445**, 523 (2007).
- [13] G. Mahmud, C. J. Campbell, K. J. M. Bishop, Y. A. Komarova, O. Chaga, S. Soh, S. Huda, K. Kandere-Grzybowska, and B. A. Grzybowski, *Nat. Phys.* **5**, 606 (2009).
- [14] D. Cubero and F. Renzoni, *Brownian Ratchets: From Statistical Physics to Bio and Nano-motors* (Cambridge University Press, Cambridge, UK, 2016).
- [15] A. V. Arzola, M. Villasante-Barahona, K. Volke-Sepúlveda, P. Jákł, and P. Zemánek, *Phys. Rev. Lett.* **118**, 138002 (2017).
- [16] A. K. Mukhopadhyay, T. Xie, B. Liebchen, and P. Schmelcher, *Phys. Rev. E* **97**, 050202(R) (2018).
- [17] J. A. Fornés, *Principles of Brownian and Molecular Motors* (Springer, Berlin, 2021).
- [18] G. G. Carlo, G. Benenti, G. Casati, and D. L. Shepelyansky, *Phys. Rev. Lett.* **94**, 164101 (2005).
- [19] B. Liebchen and P. Schmelcher, *New J. Phys.* **17**, 083011 (2015).
- [20] H. Linke, T. E. Humphrey, A. Löfgren, A. O. Sushkov, R. Newbury, R. P. Taylor, and P. Omling, *Science* **286**, 2314 (1999).
- [21] B. Lau and O. Kedem, *J. Chem. Phys.* **152**, 200901 (2020).
- [22] M. Yoshida, N. J. Ekins-Daukes, D. J. Farrell, and C. C. Phillips, *Appl. Phys. Lett.* **100**, 263902 (2012).
- [23] A. Pusch, M. Yoshida, N. P. Hylton, A. Mellor, C. C. Phillips, O. Hess, and N. J. Ekins-Daukes, *Prog. Photovolt.* **24**, 656 (2016).
- [24] T. Sogabe, C.-Y. Hung, R. Tamaki, S. Tomić, K. Yamaguchi, N. Ekins-Daukes, and Y. Okada, *Commun. Phys.* **4**, 38 (2021).
- [25] S. Denisov, L. Morales-Molina, S. Flach, and P. Hänggi, *Phys. Rev. A* **75**, 063424 (2007).
- [26] S. Flach, O. Yevtushenko, and Y. Zolotaryuk, *Phys. Rev. Lett.* **84**, 2358 (2000).
- [27] S. Denisov, S. Flach, and P. Hänggi, *Phys. Rep.* **538**, 77 (2014).
- [28] H. Schanz, M.-F. Otto, R. Ketzmerick, and T. Dittrich, *Phys. Rev. Lett.* **87**, 070601 (2001).
- [29] T. S. Monteiro, P. A. Dando, N. A. C. Hutchings, and M. R. Isherwood, *Phys. Rev. Lett.* **89**, 194102 (2002).
- [30] P. H. Jones, M. Goonasekera, D. R. Meacher, T. Jonckheere, and T. S. Monteiro, *Phys. Rev. Lett.* **98**, 073002 (2007).

- [31] E. Lundh and M. Wallin, *Phys. Rev. Lett.* **94**, 110603 (2005).
- [32] D. Poletti, G. G. Carlo, and B. Li, *Phys. Rev. E* **75**, 011102 (2007).
- [33] I. Dana, V. Ramareddy, I. Talukdar, and G. S. Summy, *Phys. Rev. Lett.* **100**, 024103 (2008).
- [34] J. Gong and P. Brumer, *Phys. Rev. E* **70**, 016202 (2004).
- [35] B. Liebchen, F. K. Diakonov, and P. Schmelcher, *New J. Phys.* **14**, 103032 (2012).
- [36] C. C. de Souza Silva, J. Van de Vondel, M. Morelle, and V. V. Moshchalkov, *Nature (London)* **440**, 651 (2006).
- [37] D. Poletti, G. Benenti, G. Casati, and B. Li, *Phys. Rev. A* **76**, 023421 (2007).
- [38] W.-L. Zhao, C.-Y. Ding, J. Liu, and L.-B. Fu, *J. Phys. B* **49**, 125303 (2016).
- [39] T. Salger, S. Kling, T. Hecking, C. Geckeler, L. Morales-Molina, and M. Weitz, *Science* **326**, 1241 (2009).
- [40] M. A. Valdez, G. Shchedrin, M. Heimsoth, C. E. Creffield, F. Sols, and L. D. Carr, *Phys. Rev. Lett.* **120**, 234101 (2018).
- [41] M. A. Valdez, G. Shchedrin, F. Sols, and L. D. Carr, *Phys. Rev. A* **99**, 063609 (2019).
- [42] S. Paul and A. Bäcker, *Phys. Rev. E* **102**, 050102(R) (2020).
- [43] B. Gutkin, *J. Phys. A* **40**, F761 (2007).
- [44] M. Akila and B. Gutkin, *J. Phys. A* **48**, 345101 (2015).
- [45] B. Dietz, T. Guhr, B. Gutkin, M. Miski-Oglu, and A. Richter, *Phys. Rev. E* **90**, 022903 (2014).
- [46] J. Che, X. Zhang, W. Zhang, B. Dietz, and G. Chai, *Phys. Rev. E* **106**, 014211 (2022).
- [47] A. J. Lichtenberg and M. A. Lieberman, *Regular and Stochastic Motion*, Applied Mathematical Sciences, Vol. 38 (Springer Science & Business Media, New York, 2013).
- [48] S. A. Gardiner, J. I. Cirac, and P. Zoller, *Phys. Rev. Lett.* **79**, 4790 (1997).
- [49] R. Sankaranarayanan, A. Lakshminarayan, and V. B. Sheorey, *Phys. Rev. E* **64**, 046210 (2001).
- [50] S. Paul, H. Pal, and M. S. Santhanam, *Phys. Rev. E* **93**, 060203(R) (2016).
- [51] S. Paul and M. S. Santhanam, *Phys. Rev. E* **97**, 032217 (2018).
- [52] G. Casati, B. V. Chirikov, F. M. Izraelev, and J. Ford, in *Stochastic Behavior in Classical and Quantum Hamiltonian Systems*, edited by G. Casati and J. Ford (Springer, Berlin, 1979), pp. 334–352.
- [53] F. M. Izraelev, *Phys. Rep.* **196**, 299 (1990).
- [54] M. S. Santhanam, S. Paul, and J. B. Kannan, *Phys. Rep.* **956**, 1 (2022).
- [55] S. Fishman, D. R. Grempel, and R. E. Prange, *Phys. Rev. Lett.* **49**, 509 (1982).
- [56] R. Lima and D. Shepelyansky, *Phys. Rev. Lett.* **67**, 1377 (1991).
- [57] A. Lakshminarayan, *Phys. Rev. E* **64**, 036207 (2001).
- [58] D. J. Tannor, *J. Chem. Educ.* **85**, 919 (2008).
- [59] J. Gong and P. Brumer, *Phys. Rev. Lett.* **97**, 240602 (2006).
- [60] A. Kenfack, J. Gong, and A. K. Pattanayak, *Phys. Rev. Lett.* **100**, 044104 (2008).
- [61] J. Wang and J. Gong, *Phys. Rev. E* **78**, 036219 (2008).
- [62] J. Pelc, J. Gong, and P. Brumer, *Phys. Rev. E* **79**, 066207 (2009).
- [63] I. Dana, *Phys. Rev. E* **81**, 036210 (2010).
- [64] B. Gadway, J. Reeves, L. Krinner, and D. Schneble, *Phys. Rev. Lett.* **110**, 190401 (2013).
- [65] A. Cao, R. Sajjad, H. Mas, E. Q. Simmons, J. L. Tanlimco, E. Nolasco-Martinez, T. Shimasaki, H. E. Kondakci, V. Galitski, and D. M. Weld, *Nat. Phys.* **18**, 1302 (2022).
- [66] J. Janarek, D. Delande, N. Cherroret, and J. Zakrzewski, *Phys. Rev. A* **102**, 013303 (2020).

Correction: The affiliations were erroneously changed during the proof production cycle and have been fixed. The institution that previously appeared as affiliation number 1 has been inserted in the footnote for author Sanku Paul as a current address.